PERGAMON

International Journal of Solids and Structures 38 (2001) 2291–2303

INTERNATIONAL JOURNAL OF SOLIDS and STRUCTURES

www.elsevier.com/locate/ijsolstr

Dynamic instability of laminated piezoelectric shell

Xin-Mai Yang *, Ya-Peng Shen

Department of Engineering Mechanics, Xi'an Jiaotong University, Xi'an, Shaanxi Province 710049, People's Republic of China

Received 12 February 1999; in revised form 16 March 2000

Abstract

In this paper, the dynamic instability of a simple supported, finite-length, laminated circular cylindrical shells subjected to parametric excitation by axial loading and covered by piezoelectric materials is presented analytically. The shell is taken to be orthotropic and could be oriented at angles of 0° and 90° (cross-ply) or at $+\theta$ and $-\theta$ (angle-ply) with respect to the shell axis. The effect of transverse shear deformation on dynamic behavior of structures has been studied, and the theory used is a general first-order shear deformation shell theory. Unimodal approximation of solution is adopted, and several mode shapes are selected to explain the effects of the piezoelectricity of materials, as well as the effects of the geometric parameters on instability regions.

Keywords: Dynamic instability; Piezoelectric shell; Mathieu's equation

1. Introduction

In recent years, smart structures with piezoelectric sensors and actuators have attracted serious attention as they can sense and alter the mechanical response during in-service operation. On the other hand, lightweight shell type structures may be one of the most popularly used structures in space vehicles. For this reason, shell type smart structures have become the focus of study for many researchers. Tzou and coworkers (1991, 1994, 1997) studied piezoelectric shell type continua using finite element method and analytical analysis method; Miller and Abramovich (1995) studied thick circular cylindrical shells with distributed self-sensing piezoelectric actuators using the first-order shear theory. Chen and Shen (1996a,b) performed the study of exact studies of piezoelectric circular cylindrical shells and piezothermoelastic shells; also, they studied the stability of piezoelectric circular cylindrical shells (Chen and Shen, 1997).

Dynamic instability of circular cylinders has been studied by many researchers. The parametric resonance of cylindrical shells under axial loads was first treated by Bolotin (1964), Yao (1963, 1965) and Tamura (1975), etc. For thin cylindrical shells under periodic axial loads, the method of solution is usually first to reduce the equation of motion to a system of Methieu's equations. Bert and Birman (1998) studied the parametric instability of thick, orthotropic, circular cylindrical shells using first-order shear deformable shell theory. The perturbation method is employed by Argento and Scott (1993a,b) in the study of dynamic

* Corresponding author.

0020-7683/01/$ - see front matter
PII: S0020-7683(00)00119-0

instability of layered anisotropic circular cylindrical shells. In a recent study, Ng et al. (1998) investigated the effects of different lamination schemes of antisymmetric cross-ply laminates on the instability regions of the laminated cylindrical shells. Lam and Ng (1997) studied the dynamic stability of thin isotropic cylindrical shells using four common thin shell theories, namely, the Donnell, Love, Sanders and Flugge shell theories. Up to now, to the authors' knowledge, however, there is no paper published about the dynamic instability of piezoelectric circular cylindrical shells.

In this paper, dynamic instability of a simple supported, finite-length, laminated circular cylindrical shells covered by piezoelectric materials, which are distributed symmetrically, is studied. The shell is subjected to a uniformly distributed cyclic axial loading and includes the effects of transverse shear deformation. The effect of the piezoelectric effect on the dynamic instability is considered. The result can be useful in an active control.

2. Assumptions

The analysis is based on the following assumptions, most of which can be found in Bert and Birman (1998):

1. The analysis is linear, including both linear constitutive relations for the material and linear strain–displacement relations.
2. The shell is circular cylindrical without initial imperfections.
3. The in-surface and rotary inertia are neglected.
4. The loading considered is axial, assumed to be uniformly distribution and to consist of a constant portion and a simple harmonic excitation over the end sections.
5. Perfect bonding is considered between different layers.
6. The directions of polarization of piezoelectric layers are in the same direction.
7. All damping effects are neglected.
8. The unimodal approximation of solution is adopted, and several isolated dynamic instability mode shapes are analyzed in numerical examples in order to take account of the effect of piezoelectricity.

3. Analysis

Consider an orthotropic circular cylindrical cross-ply laminated shell covered by a piezoelectric material symmetrically. The shell is subjected to uniformly distributed, parametric, time-dependent loads of intensity $N_1(t)$ along the axial direction. According to Love's and Loo's theory, the equations of motion of such a shell are (the effect of in-surface and rotary inertias has been neglected)

$$N_{1,x} + N_{6,y} = 0, \tag{1}$$

$$N_{6,x} + N_{2,y} + \frac{1}{R}Q_4 = 0, \tag{2}$$

$$Q_{5,x} + Q_{4,y} - \frac{N_2}{R} + N_1^0(t)w_{,xx} = \rho h w_{,tt}, \tag{3}$$

$$M_{1,x} + M_{6,y} - Q_5 = 0, \tag{4}$$

$$M_{6,x} + M_{2,y} - Q_4 = 0. \tag{5}$$

The charge equilibrium equation is

$$D_{z,z} + D_{y,y} + D_{x,x} + \frac{1}{R} D_z = 0, \tag{6}$$

where M_i and N_i denote the stress couples and in-surface stress resultants respectively; Q_{ij} are the shearing stress resultants; u, v, w, the displacements along the x-axis (axial), y-axis (circumferential), z-axis (radial), respectively, ψ_1 and ψ_2, the bending slopes in the x–z and y–z planes, t is the time, $(\ldots)_{,i} \equiv \partial(\ldots)/\partial i$, ρ is the material density, and D_i is the electric displacement along the i-axis.

Suppose the voltage distribution is $\phi = z\phi_0(x, y)$. The constitutive equations of a specially material are

$$\begin{Bmatrix} N_1 \\ N_2 \\ N_6 \\ M_1 \\ M_2 \\ M_6 \end{Bmatrix} = \begin{bmatrix} A_{11} & A_{12} & 0 & 0 & 0 & 0 \\ A_{12} & A_{22} & 0 & 0 & 0 & 0 \\ 0 & 0 & A_{66} & 0 & 0 & 0 \\ 0 & 0 & 0 & D_{11} & D_{12} & 0 \\ 0 & 0 & 0 & D_{12} & D_{22} & 0 \\ 0 & 0 & 0 & 0 & 0 & D_{66} \end{bmatrix} \begin{Bmatrix} \varepsilon_1^0 \\ \varepsilon_2^0 \\ \varepsilon_6^0 \\ \chi_1 \\ \chi_2 \\ \chi_6 \end{Bmatrix} - \begin{bmatrix} c_{31} \\ c_{32} \\ 0 \\ f_{31} \\ f_{32} \\ 0 \end{bmatrix} \{-\phi_0\}. \tag{7}$$

The extensional, coupling, and bending stiffness are defined as

$$(A_{ij}, D_{ij}) = \int_{-h/2}^{h/2} (1, z^2) Q_{ij}\, \mathrm{d}z + \int_{h/2}^{h/2+h_p} (1, z^2) E_{ij}\, \mathrm{d}z + \int_{-h/2-h_p}^{-h/2} (1, z^2) E_{ij}\, \mathrm{d}z, \tag{8}$$

$$\begin{aligned} (c_{ij}, f_{ij}) &= \int_{h/2}^{h/2+h_p} (1, z) e_{ij}\, \mathrm{d}z + \int_{-h/2-h_p}^{-h/2} (1, z) e_{ij}\, \mathrm{d}z, \\ \varepsilon_{ij} &= \int_{h/2}^{h/2+h_p} z\varepsilon_{ij}\, \mathrm{d}z + \int_{-h/2-h_p}^{-h/2} z\varepsilon_{ij}\, \mathrm{d}z, \end{aligned} \tag{9}$$

where, E_{ij} are the modulus of the piezoelectric film PVDF, and h_p, the thickness of the PVDF, Q_{ij}, the plane-stress transformed reduced elastic stiffness, and ε_{ij}, e_{ij}, the dielectric constant and piezoelectric stress coefficient, respectively. The shear stress resultants are

$$\begin{Bmatrix} Q_4 \\ Q_5 \end{Bmatrix} = \begin{bmatrix} S_{44} & 0 \\ 0 & S_{55} \end{bmatrix} \begin{Bmatrix} \varepsilon_4 \\ \varepsilon_5 \end{Bmatrix} + \begin{bmatrix} 0 & f_{24} \\ f_{15} & 0 \end{bmatrix} \begin{Bmatrix} \phi_{0,x} \\ \phi_{0,y} \end{Bmatrix}, \tag{10}$$

where the thickness shear stiffnesses are

$$S_{ii} = k_i^2 \int_{-h/2}^{h/2} Q_{ii} \quad (i = 4, 5) \tag{11}$$

and k_i^2 is the shear correction coefficient. The electric displacement resultants are

$$\begin{Bmatrix} D_x \\ D_y \\ D_z \end{Bmatrix} = \begin{bmatrix} 0 & 0 & 0 & e_{15} & 0 \\ 0 & 0 & e_{24} & 0 & 0 \\ e_{31} & e_{32} & 0 & 0 & 0 \end{bmatrix} \begin{Bmatrix} \varepsilon_1^0 \\ \varepsilon_2^0 \\ \varepsilon_4 \\ \varepsilon_5 \\ \varepsilon_6^0 \end{Bmatrix} + \begin{bmatrix} \varepsilon_{11} & & \\ & \varepsilon_{22} & \\ & & \varepsilon_{33} \end{bmatrix} \begin{Bmatrix} -z\phi_{0,x} \\ -z\phi_{0,y} \\ -\phi_0 \end{Bmatrix}. \tag{12}$$

In the above equations, ε_i^0 are the middle-surface engineering strain components, ε_4 and ε_5, the transverse shear strains, and χ_i, the curvature and twist changes given by

$$\varepsilon_1^0 = u_{,x}, \quad \varepsilon_2^0 = v_{,y} + w/R,$$

$$\varepsilon_6^0 = u_{,y} + v_{,x},$$

$$\varepsilon_4 = \psi_2 + w_{,y} - \frac{v}{R}, \quad \varepsilon_5 = \psi_1 + w_{,x}, \tag{13}$$

$$\chi_1 = \psi_{1,x}, \quad \chi_2 = \psi_{2,y},$$

$$\chi_6 = \psi_{1,y} + \psi_{2,x} + (v_{,x} - u_{,y})/2R.$$

Because of the symmetric arrangement of the PVDF, the relationship of voltage of the two piece of PVDF is

$$\phi^{\text{up}} = -\phi^{\text{down}}. \tag{14}$$

So, the even term of z which related with ϕ will be zero when the integral is along z-axis.

The shell is freely supported. The boundary conditions considered in Tamura and Babcock (1975) are used:

$$N_1(0,y) = N_1(L,y) = 0, \quad v(0,y) = v(L,y) = 0,$$

$$M_1(0,y) = M_1(L,y) = 0, \quad \psi_2(0,y) = \psi_2(L,y) = 0, \tag{15}$$

$$w(0,y) = w(L,y) = 0,$$

and the electric boundary conditions

$$\phi(0,y) = \phi(L,y) = 0. \tag{16}$$

If the shell is a cylindrical curved panel (open shell) freely supported, which requires that the following additional boundary conditions be satisfied (Tamura and Babcock, 1975):

$$N_2(x,0) = N_2(x,b) = 0, \quad M_2(x,0) = M_2(x,b) = 0,$$

$$w(x,0) = w(x,b) = 0, \quad u(x,0) = u(x,b) = 0, \tag{17}$$

$$\psi_1(x,0) = \psi_1(x,b) = 0, \quad \phi(x,0) = \phi(x,b) = 0.$$

The boundary conditions (14) and (15) are satisfied if

$$u = U(t)h\sin\alpha x\cos\beta y, \quad \psi_1 = X(t)\cos\alpha x\sin\beta y,$$

$$v = V(t)h\cos\alpha x\sin\beta y, \quad \psi_2 = Y(t)\sin\alpha x\cos\beta y, \tag{18}$$

$$w = W(t)h\sin\alpha x\sin\beta y, \quad \phi_0 = \Phi(t)h\sin\alpha x\sin\beta y,$$

where $\alpha \equiv m\pi/L$ and $\beta \equiv n/R$ for a complete cylinder and $n\pi/b$ for a panel.

The effect of in-surface and rotary inertias on vibration of the shell at frequencies near the fundamental frequency are negligible. Since dynamic stability is most important in the case in which the excitation frequencies are of the same order as the fundamental frequency, these inertias are neglected here. Substituting Eqs. (7), (10), (12) and (18) into Eqs. (1)–(6) and integrating Eq. (6) along the z-axis, one can obtain the following set of equations:

$$[C_{ij}]\{U,V,W,X,Y,\Phi\}^{\mathrm{T}} = \left\{0,0,\frac{\rho h^2}{E_T}W_{,tt},0,0,0\right\}^{\mathrm{T}}. \tag{19}$$

The nondimensional coefficients of the square matrix C_{ij} are

$$C_{11} = -A_{11}\alpha^2 - A_{66}\beta^2, \quad C_{12} = C_{21} = -\alpha\beta(A_{12} + A_{66}),$$

$$C_{13} = C_{31} = \alpha(h/R)A_{12}, \quad C_{14} = C_{41} = 0,$$

$$C_{15} = C_{51} = 0, \quad C_{16} = 0,$$

$$C_{22} = -A_{66}\alpha^2 - A_{22}\beta^2 - (h/R)^2 S_{44},$$

$$C_{23} = C_{32} = (S_{44} + A_{22})(h/R)\beta, \quad C_{24} = C_{42} = 0,$$

$$C_{25} = C_{52} = (h/R)S_{44}, \quad C_{26} = (f_{24}/E_T R)\beta,$$

$$C_{33} = -S_{55}\alpha^2 - S_{44}\beta^2 - (h/R)^2 + N_1^0\alpha^2\cos 2\omega t,$$

$$C_{34} = C_{43} = -S_{55}\alpha, \quad C_{35} = C_{53} = -S_{44}\beta,$$

$$C_{36} = -\frac{f_{15}\alpha^2}{hE_T} - \frac{f_{24}\beta^2}{hE_T}, \quad C_{44} = -D_{11}\alpha^2 - D_{66}\beta^2 - S_{55},$$

$$C_{45} = C_{54} = -(D_{12} + D_{66})\alpha\beta, \quad C_{46} = \frac{f_{31} - f_{15}}{hE_T}\alpha,$$

$$C_{55} = -D_{66}\alpha^2 - D_{22}\beta^2 - S_{44}, \quad C_{56} = \frac{f_{32} - f_{24}}{hE_T}\beta,$$

$$C_{61} = -(c_{31}/R)\alpha, \quad C_{62} = (c_{24}/R)\beta - (c_{32}/R)\beta,$$

$$C_{63} = -(c_{15}/h)\alpha^2 - (c_{24}/h)\beta^2 + c_{32}h/R^2, \quad C_{65} = (-c_{24} - c_{32})\beta/h,$$

$$C_{64} = (-c_{15} - c_{31})\alpha/h, \quad C_{66} = (\varepsilon_{11}/h)\alpha^2 + (\varepsilon_{22}/h)\beta^2,$$

where,

$$A_{ij} = \frac{A_{ij}}{E_T h}, \quad S_{ij} = \frac{S_{ij}}{E_T h}, \quad D_{ij} = \frac{D_{ij}}{E_T h^3},$$
$$\alpha = \frac{m\pi h}{L}, \quad \beta = \frac{nh}{R}, \quad N_1^0 = N_1^0/E_T h.$$

Representing the nondimensional x-axis force by

$$N_1^0 = N_0 + N_1\cos 2\omega t, \tag{20}$$

where N_0 is a constant portion and always set to zero in the next few sections. N_1 is the swing of the simple harmonic excitation. Then, the set (18) can be reduced to a single linear second-order differential equation as follows:

$$W_{,\tau\tau} + (a_0 - 2q\cos 2\tau)W = 0. \tag{21}$$

This is the well-known Mathieu's equation, where τ is a nondimensional time parameter ($=\omega t$), and the Mathieu parameters are

$$
\begin{aligned}
&a_0 = (1/\varpi^2)(L/h)^4 K_w, \quad q = (1/2\varpi^2)(L/h)^4 N_1\alpha^2,\\
&\varpi^2 = (\rho L^4/E_T h^2)\omega^2,\\
&K_w = -(C_{13}K_U + C_{23}K_V + C_{34}K_X + C_{35}K_Y + C_{36}K_\Phi) + \alpha^2 S_{55} + \beta^2 S_{44} + \left(\frac{h}{R}\right)^2 A_{22} + N_0\alpha^2,\\
&K_\Phi = -C_{34} + \frac{C_{44}K_X}{C_{46}} + C_{45}K_Y, \quad K_U = -\frac{C_{12}K_V + C_{13}}{C_{11}}, \quad K_V = -B_{12} + \frac{B_{13}K_X}{B_{11}} + B_{14}K_Y,\\
&K_Y = -\frac{D_1 + D_2K_X}{D_3}, \quad K_X = \frac{D_4D_3 - D_1D_6}{D_2D_6 - D_5D_3},\\
&D_1 = B_{12}B_{21} - B_{22}B_{11}, \quad D_2 = B_{13}B_{21} - B_{23}B_{11},\\
&D_3 = B_{14}B_{21} - B_{24}B_{11}, \quad D_4 = B_{12}B_{31} - B_{32}B_{11},\\
&D_5 = B_{13}B_{31} - B_{33}B_{11}, \quad D_6 = B_{14}B_{31} - B_{24}B_{11},\\
&B_{11} = -\frac{C_{12}^2C_{46}}{C_{11}} + C_{22}C_{46}, \quad B_{12} = -\frac{C_{12}C_{13}C_{46}}{C_{11}} + C_{23}C_{46} - C_{34}C_{26},\\
&B_{13} = C_{25}C_{46} - C_{45}C_{26}, \quad B_{14} = -C_{44}C_{26},\\
&B_{21} = C_{25}C_{46}, \quad B_{22} = C_{35}C_{46} - C_{34}C_{56},\\
&B_{23} = C_{45}C_{46} - C_{44}C_{56}, \quad B_{24} = C_{55}C_{46} - C_{45}C_{56},\\
&B_{31} = C_{62}C_{46} - \frac{C_{12}C_{61}C_{46}}{C_{11}}, \quad B_{32} = C_{63}C_{46} - C_{34}C_{66} - \frac{C_{13}C_{61}C_{46}}{C_{11}},\\
&B_{33} = C_{64}C_{46} - C_{44}C_{66}, \quad B_{34} = C_{65}C_{46} - C_{45}C_{66}.
\end{aligned}
\tag{22}
$$

The boundary of the instability regions of the solutions of Mathieu's equation are tabulated. The boundary of the first instability region are given by McLachlan (1964)

$$a_0 = 1 \mp q - \tfrac{1}{8}q^2 \pm \tfrac{1}{64}q^3 - \cdots \tag{23}$$

if q is small enough so that the series converges. The higher instability regions are not always realized if the shell vibrates with limited amplitudes due to damping.

It is convenient to show the boundary of the instability regions on the frequency–load plane where the horizontal axis corresponds to the squared nondimensional frequency ω^2 and the vertical axis represents the nondimensional amplitude of the load N_1.

If the term q is so small that nonlinear terms in Eq. (22) can be neglected, the boundaries of the first instability region are represented by the following relations:

$$\omega^2 = (L/h)^4\left(K_w \mp \tfrac{1}{2}N_1\alpha^2\right). \tag{24}$$

4. Results and discussion

A two-layer cross-ply shell is considered. The material properties taken were the following:

$$E_L/E_T = 40, \quad G_{LT}/E_T = G_{LZ}/E_T = 0.6, \quad G_{TZ}/E_T = 0.5, \quad \nu_{LT} = 0.25, \quad k_4^2 = k_5^2 = \tfrac{5}{6},$$
$$E_T = 6.85 \times 10^9 \text{ Pa}.$$

The dimension of the shell

$$h = 0.02 \text{ m}, \quad b/R = \theta = \frac{\pi}{6}.$$

For the shell without a piezoelectric material, the dimensionless stretching, bending, and transverse shear stiffness are as follows (Bert and Birman, 1998): $A_{11} = 20.5$, $A_{12} = 0.25$, $A_{22} = 20.5$, $A_{66} = 0.6$, $D_{11} = 1.7083$, $D_{12} = 0.07083$, $D_{22} = 1.7083$, $D_{66} = 0.05$, $S_{44} = 0.4583$, $S_{55} = 0.4583$. The material properties of the PVDF are taken as $e_{31} = 0.044$ C/m^2, $\varepsilon_{11} = 0.1 \times 10^{-9}$ F/m, $\varepsilon_{22} = 0.1 \times 10^{-9}$ F/m, $\rho = 1800$ kg/m^3 $E_{11} = E_{22} = 2 \times 10^9$ Pa, $G_{12} = G_{13} = 0.775 \times 10^9$ Pa, $G_{23} = 0.775 \times 10^9$ Pa. The thickness of PVDF, $h_p = 50$ μm. Let $\beta = n\pi/b$, the method in Bert and Birman (1998) can be used for the calculation of the dynamic instability of a cylindrical panel, a comparable result can be obtained.

Figs. 1–4 present the boundaries of instability regions corresponding to different mode shapes and different shells. In these figures, the boundaries of instability regions which consider the effect of PVDF and which do not consider the effect of PVDF are almost overlapped; this claims that the effect of PVDF is very slight. In general, we believe that the piezoelectric effect should increase the frequency of structures, but, in this case, we notice that the dynamic instability frequency is slightly decreased due to the piezoelectric effect. The result is very interesting although the effect is slight, and perhaps it is owing to the symmetric distribution of PVDF.

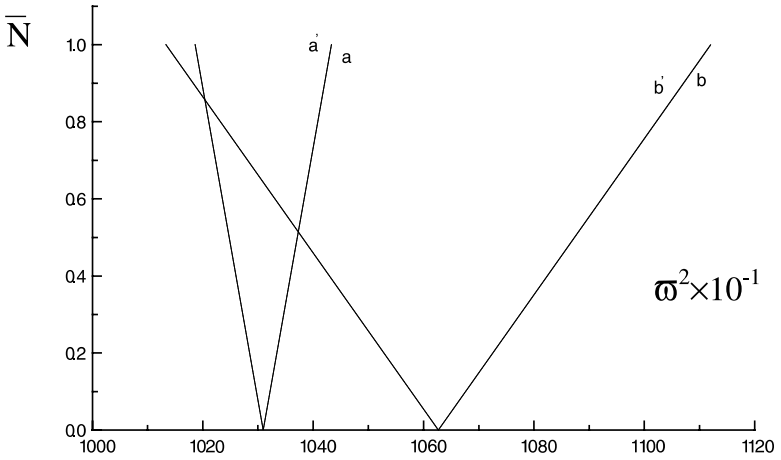

Fig. 1. $L/R = 1$, $R/H = 5$, a, b (solid) for $(m, n) = (1, 5)$, $(2, 5)$ without PVDF, respectively, and a′, b′ (dash) for the case with PVDF.

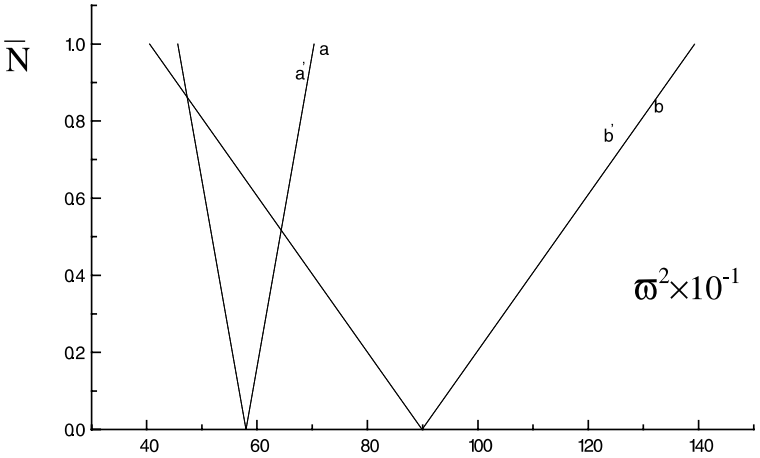

Fig. 2. $L/R = 1$, $R/H = 5$, a, b (solid) for $(m, n) = (1, 0)$, $(2, 0)$ without PVDF, respectively, and a′, b′ (dash) for the case with PVDF.

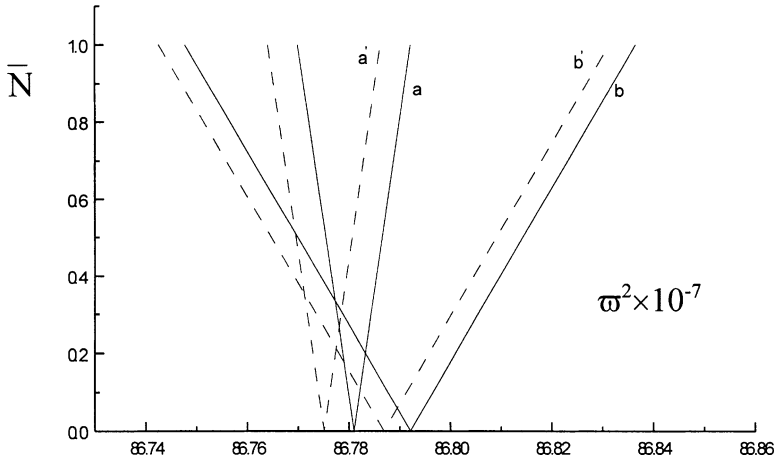

Fig. 3. $L/R = 10$, $R/H = 15$, a, b (—) for $(m, n) = (1, 5), (2, 5)$ without PVDF, respectively, and a′, b′ (- - -) for the case with PVDF.

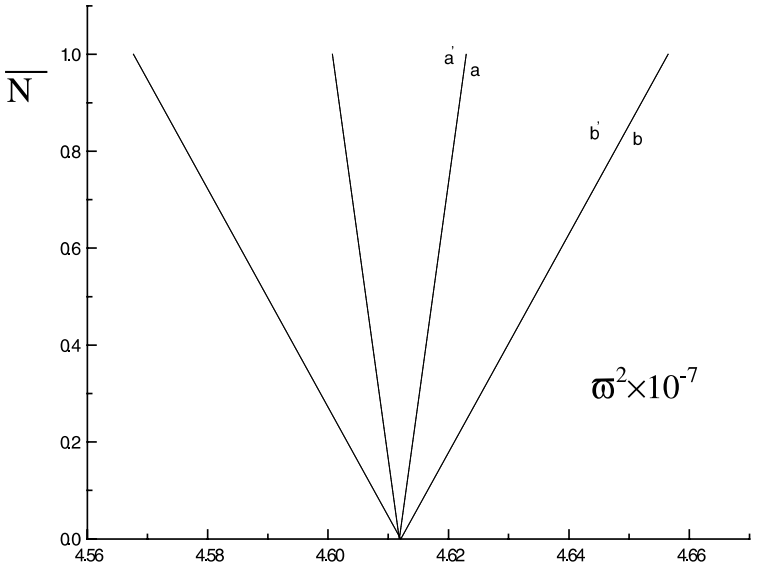

Fig. 4. $L/R = 10$, $R/H = 15$, a, b (—) for $(m, n) = (1, 0), (2, 0)$ without PVDF, respectively, and a′, b′ (- - -) for the case with PVDF.

Table 1 presents a comparable result of a short thick cylindrical panel ($L/R = 1,\ R/H = 5$), and Table 2 presents the result of a long thin cylindrical panel ($L/R = 10,\ R/H = 15$). Four mode shapes are considered here, it is $m = 1$ and 2 (m is the number of half waves along the shell axis), $n = 0$ and 5 (n is the number of circumferential half waves), where L stands for including piezoelectric layers but ignoring piezoelectric effect, and P stands for considering piezoelectric effect.

From the result of calculation, one can draw a conclusion: To short thick shell, the PVDF hardly affects the dynamic instability. If the precision is improved enough, then, to long thin shell, the dynamic instability frequency is slightly waned due to the piezoelectric effect.

When using PVDF as actuators, it is equivalent to applying the load. Theoretically, the size of instability zone and instability frequency can be altered freely. There is, however, almost no variation of dimensionless

Table 1
Effect of PVDF on a short, thick shell ($L/R = 1$, $R/H = 5$)

m	n	$\varpi_0^2 \times 10^{-3}$ ($\bar{N}_1 = 0$)		$\varpi_1^2 \times 10^{-3}$ ($\bar{N}_1 = 1$)		$\varpi_2^2 \times 10^{-3}$ ($\bar{N}_1 = 1$)	
		Without	With	Without	With	Without	With
1	5	10.3094	10.3095	10.1860	10.1861	10.4328	10.4328
1	0	0.57975	0.57975	0.45638	0.45638	0.70312	0.70312
2	5	10.6268	10.6269	10.1333	10.1335	11.1203	11.1204
2	0	0.89906	0.89906	0.40558	0.40558	1.39254	1.39254

Table 2
Effect of PVDF on a long thin shell ($L/R = 10$, $R/H = 15$)

m	n	$\varpi_0^2 \times 10^{-7}$ ($\bar{N}_1 = 0$)		$\varpi_1^2 \times 10^{-7}$ ($\bar{N}_1 = 1$)		$\varpi_2^2 \times 10^{-7}$ ($\bar{N}_1 = 1$)	
		Without	With	Without	With	Without	With
1	5	86.7810	86.7751	86.7699	86.7640	86.7921	86.7862
1	0	4.61183	4.61184	4.60073	4.60073	4.62293	4.62294
2	5	86.7921	86.7869	86.7477	86.7425	86.8365	86.8313
2	0	4.61208	4.61208	4.56767	4.56767	4.65649	4.65649

dynamic instability frequency until the voltage reaches 10^{11} V; the voltage will cause the electric field which will damage the PVDF.

If by using the piezoelectric ceramic PZT, the result is different from using PVDF because its modulus and piezoelectric constant are greater than PVDF's. Figs. 5–8 reveal the boundaries of instability regions

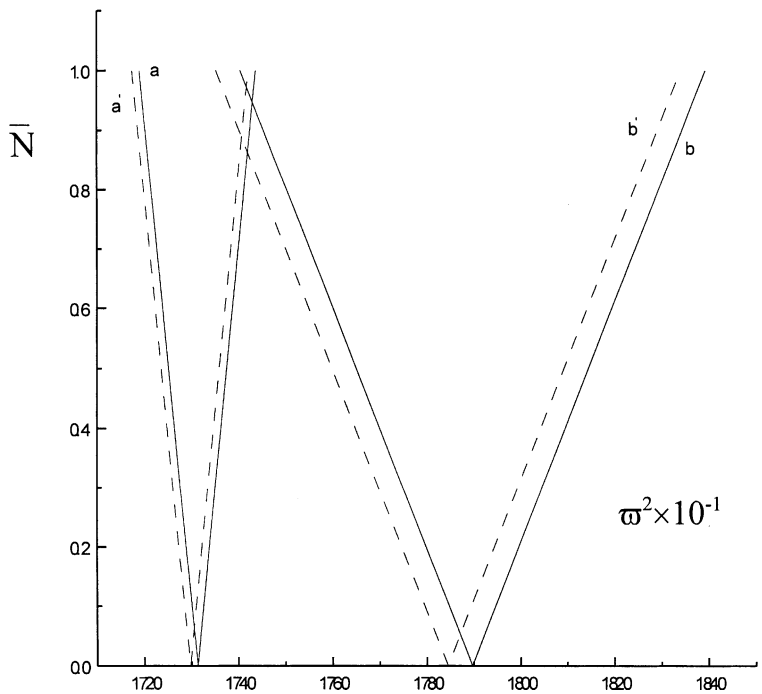

Fig. 5. $L/R = 1$, $R/H = 5$ a, b (—) for $(m, n) = (1, 5)$, $(2, 5)$ (ignoring piezoelectric effect) and a′, b′ (- - -) for the case considering piezoelectric effect.

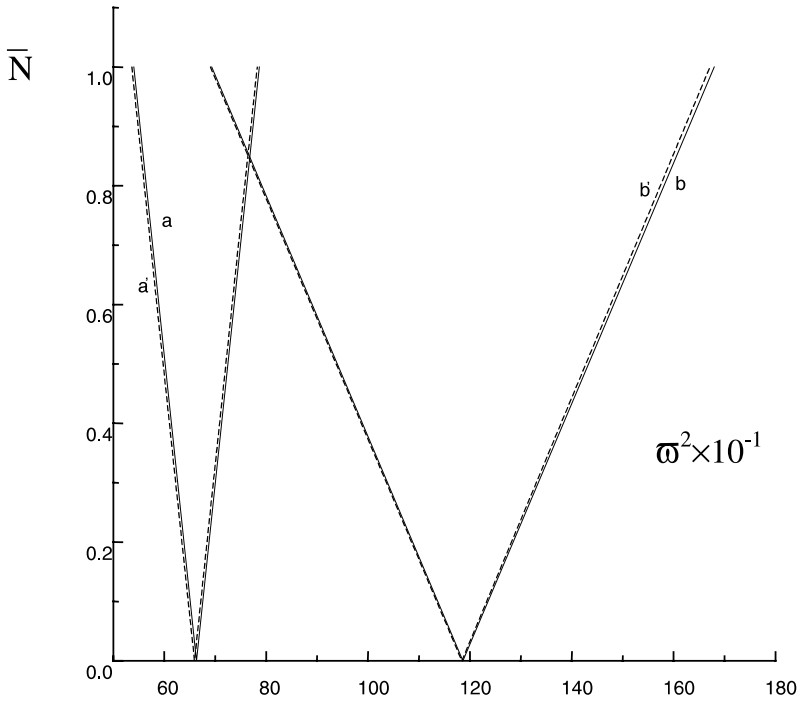

Fig. 6. $L/R = 1$, $R/H = 5$ a, b (—) for $(m, n) = (1, 0)$, $(2, 0)$ (ignoring piezoelectric effect) and a′, b′ (- - -) for the case considering piezoelectric effect.

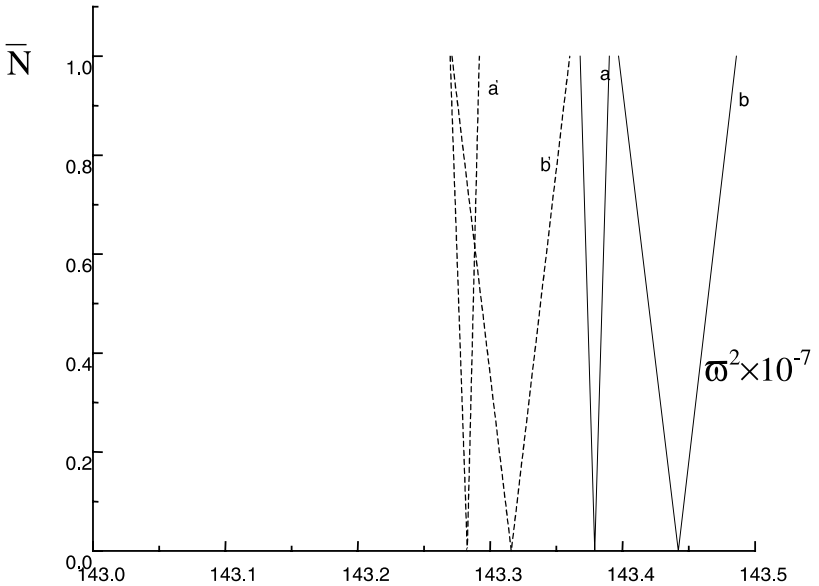

Fig. 7. $L/R = 10$, $R/H = 15$ a, b (—) for $(m, n) = (1, 5)$, $(2, 5)$ (ignoring piezoelectric effect) and a′, b′ (- - -) for the case considering piezoelectric effect.

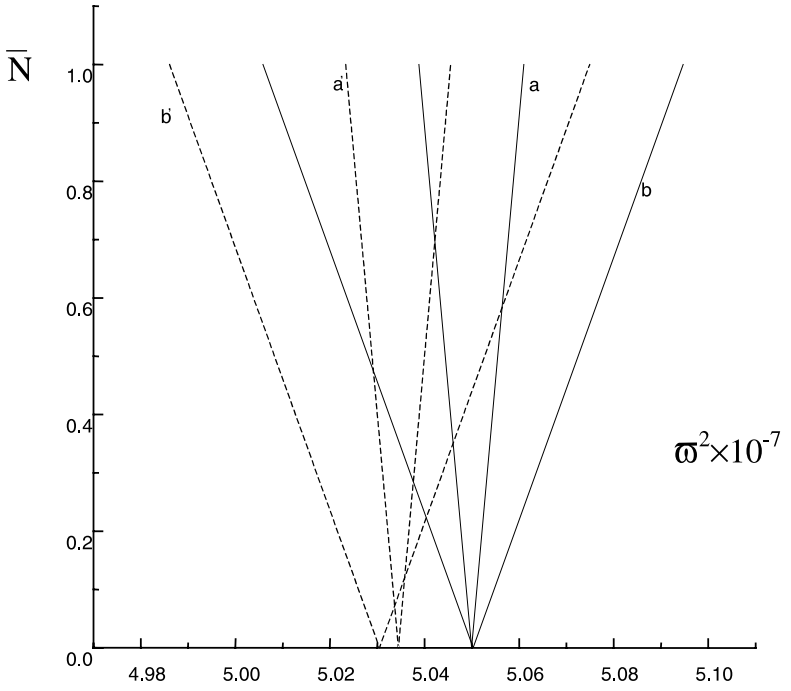

Fig. 8. $L/R = 10$, $R/H = 15$ a, b (—) for $(m,n) = (1,0), (2,0)$ (ignoring piezoelectric effect) and a′, b′ (- - -) for the case considering piezoelectric effect.

corresponding to different mode shapes and shells. From the result, the piezoelectric effect of PZT causes the instability frequency to decrease.

Tables 3 and 4 present a comparable result of different shells for different modes. The comparison clearly shows that the effect of PZT is very slight. Material properties of the PZT used in Tables 3 and 4 are as follows:

Table 3
Effect of PZT on a short, thick shell ($L/R = 1$, $R/H = 5$)

m	n	$\varpi_0^2 \times 10^{-3}$ ($\bar{N}_1 = 0$)		$\varpi_1^2 \times 10^{-3}$ ($\bar{N}_1 = 1$)		$\varpi_2^2 \times 10^{-3}$ ($\bar{N}_1 = 1$)	
		L	P	L	P	L	P
1	5	17.3131	17.2974	17.1897	17.1741	17.4365	17.4208
1	0	0.66323	0.65920	0.53986	0.53583	0.78660	0.78257
2	5	17.8972	17.8454	17.4037	17.3519	18.3906	18.3388
2	0	1.18642	1.18425	0.69294	0.69077	1.67990	1.67173

Table 4
Effect of PVDF on a long thin shell ($L/R = 10$, $R/H = 15$)

m	n	$\varpi_0^2 \times 10^{-7}$ ($\bar{N}_1 = 0$)		$\varpi_1^2 \times 10^{-7}$ ($\bar{N}_1 = 1$)		$\varpi_2^2 \times 10^{-7}$ ($\bar{N}_1 = 1$)	
		L	P	L	P	L	P
1	5	143.379	143.281	143.368	143.270	143.390	143.292
1	0	5.04993	5.03446	5.03882	5.02336	5.06103	5.04556
2	5	143.442	143.316	143.397	143.271	143.486	143.360
2	0	5.05026	5.03049	5.00584	4.98607	5.09467	5.07490

$$[C] = \begin{bmatrix} 13.90 & 7.78 & 7.43 & & & \\ 7.78 & 13.90 & 7.43 & & & \\ 7.43 & 7.43 & 11.50 & & & \\ & & & 2.56 & & \\ & & & & 2.56 & \\ & & & & & 3.06 \end{bmatrix} \times 10^{10} \text{ Pa},$$

$$e_{31} = e_{32} = -5.20 \text{ C/m}^2, \quad \rho = 7.5 \times 10^3 \text{ kg/m}^3, \quad h_p = 0.001 \text{ m},$$
$$\varepsilon_{11} = \varepsilon_{22} = 730\varepsilon_0, \quad \varepsilon_{33} = 635\varepsilon_0,$$

where $\varepsilon_0 = 8.854 \times 10^{-12}$ F/m and other terms not shown here are assumed to be zero.

When using PZT as actuators, the effect of piezoelectric is notable compared with PVDF due to the higher piezoelectric constant. But the voltage still reaches 10^8 V. It is obviously too high to work for PZT.

5. Conclusion

Comparison of the effect of PZT and PVDF shows that PZT has a stronger effect than PVDF. However, neither PZT nor PVDF has a strong effect on the unstable region of the structure. Dynamic instability regions mainly depend on the mechanic load.

Acknowledgements

The study was supported by the National Natural Science Foundation (59635140).

References

Argento, A., Scott, R.A., 1993a. Dynamic instability of layered anisotropic circular cylindrical shells, Part I: theoretical development. Journal of Sound and Vibration 162, 311–322.

Argento, A., Scott, R.A., 1993b. Dynamic instability of layered anisotropic circular cylindrical shells, Part II: numerical results. Journal of Sound and Vibration 162, 323–332.

Bert, C.W., Birman, V., 1998. Parametric instability of thick orthotropic circular cylindrical shells. Acta Mechanics 71, 61–76.

Bolotin, V.V., 1964. The Dynamic Stability of Elastic Systems. Holden-Day, San Francisco.

Chen, C.Q., Shen, Y.P., 1996a. Piezothermoelasticity Analysis for circular cylindrical shell under the state of axisymmetric deformation. International Journal of Engineering Science 34, 1585–1600.

Chen, C.Q., Shen, Y.P., Wang, X.M., 1996b. Exact solution of orthotropic cylindrical shell with piezoelectric layers under cylindrical bending. International Journal of Solid and Structures 33, 4481–4494.

Chen, C.Q., Shen, Y.P., 1997. Stability analysis of piezoelectric circular cylindrical shells. ASME Journal of Applied Mechanics 64, 847–862.

Lam, K.Y., Ng, T.Y., 1997. Dynamic stability of cylindrical shells subjected to conservative periodic axial loads using different shell theories. Journal of Sound and Vibration 207, 497–520.

McLachlan, N.W., 1964. Theory and application of Mathieu functions. Dover, New York.

Miller, S.E., Abramovich, H., 1995. A self-sensing piezolaminated actuator model for shells using a shear deformation theory. Journal of Intelligent Material Systems and Structures 6, 624–638.

Ng, T.Y., Lam, K.Y., Reddy, J.N., 1998. Dynamic stability of cross-ply laminated composite cylindrical shells. International Journal of Mechanics Science 40, 805–823.

Tamura, Y.S., Babcock, C.D., 1975. Dynamic stability of cylindrical shells under step loading. ASME Journal of Applied Mechanics 190-194.

Tzou, H.S., Tseng, C.L., 1991. Distributed modal identification and vibration control of continua: piezoelectric element formation and analysis. Journal of Dynamic Systems Measurement and Control 113, 500–505.

Tzou, H.S., Zhong, J.P., Holkamp, J.J., 1994. Spatially distributed orthogonal piezoelectric shell actuators: theory and application. Journal of Sound and Vibration 177, 363–378.

Tzou, H.S., Boa, Y., 1997. Nonlinear piezothermoelastic shell laminates. ASME Journal of Vibration and Acoustics 119, 374–381.

Yao, J.C., 1963. Dynamic stability of cylindrical shells under static and periodic axial and radial loads. AIAA Journal 1, 1391–1396.

Yao, J.C., 1965. Nonlinear elastic bucking and parametric excitation of a cylinder under axial loads. ASME Journal of Applied Mechanics 32, 109–115.